

LETTERS

Femtosecond Infrared and Visible Spectroscopy of Photoinduced Intermolecular Electron Transfer Dynamics and Solvent–Solute Reaction Geometries: Coumarin 337 in Dimethylaniline[†]

Chengfei Wang, Boris Akhremitchev, and Gilbert C. Walker*

Department of Chemistry, University of Pittsburgh, Pittsburgh, Pennsylvania 15260

Received: September 11, 1996; In Final Form: January 23, 1997[⊗]

We present time-resolved infrared and visible spectroscopic data that reveal the relative orientations of donor and acceptor molecules in the $\langle\tau_{\text{ET}}\rangle = 4$ ps intermolecular electron transfer between dimethylaniline solvent and coumarin 337 solute. Although consideration of the dipolar attraction suggests the two species are most likely to be aligned with their molecular long axes parallel, the electron transfer occurs between species with their long axes perpendicular.

Introduction

Much recent research has focused on the coupling between solvent and solute degrees of freedom in chemical reactions.¹ The solvent through polarization or collisions influences the charge rearrangements that accompany solution reactions. The solute–solvent interactions are typically treated under linear response, which implies that the associated motions are harmonic. In an effort to obtain molecular information on the nature of the solute–solvent environment, theory^{2–11} and experimental^{12–23} observations of solvation and electron transfer (ET) dynamics have been avidly pursued. Efforts are focusing on the role of nonequilibrium configurations of the solvent and the solute in electron transfer. Of particular interest are the dynamics along these configurational coordinates and the transition from solvent controlled to vibrationally controlled ET.

Recent theoretical and experimental results indicate that first-shell solvent molecules provide the majority of stabilization energy in condensed phase reactions.^{23–25} Intermolecular charge transfer reactions between a solute and a solvent may provide

a direct probe of the first solvent shell because of the rapid decay with distance of the electron-tunneling probability. We report spectroscopic measurements of the relative orientation of the donor–acceptor pair in an ET reaction.

Experimental Section

High-purity solvents and solutes were purchased from Aldrich and were used without further purification. Samples were prepared at 10^{-6} M for static fluorescence and 10^{-3} M for absorption spectroscopy.

The pump–probe spectrometer has been described in detail elsewhere.²⁶ It is tunable from 50 000 to 1000 cm^{-1} . The sample is placed in a spinning sample cell that provides a fresh sample volume for every laser shot. The 400 nm excitation energy was 300 nJ/pulse, with a pump spot diameter of 200 μm and a path length of 200 μm .

Results

The molecules of interest, coumarin 337 (C337) and dimethylaniline (DMA), are shown in Chart 1.

When C337 is dissolved in solvents of similar polarity as that of DMA, optical excitation into the lowest excited singlet electronic state (S_1) results in strong fluorescence. On the other hand, when solution of C337 in DMA is similarly optically

[†] This work has been supported by 3M Company, the Petroleum Research Fund, and ONR.

* Author to whom correspondence should be addressed.

[⊗] Abstract published in *Advance ACS Abstracts*, April 1, 1997.

CHART 1

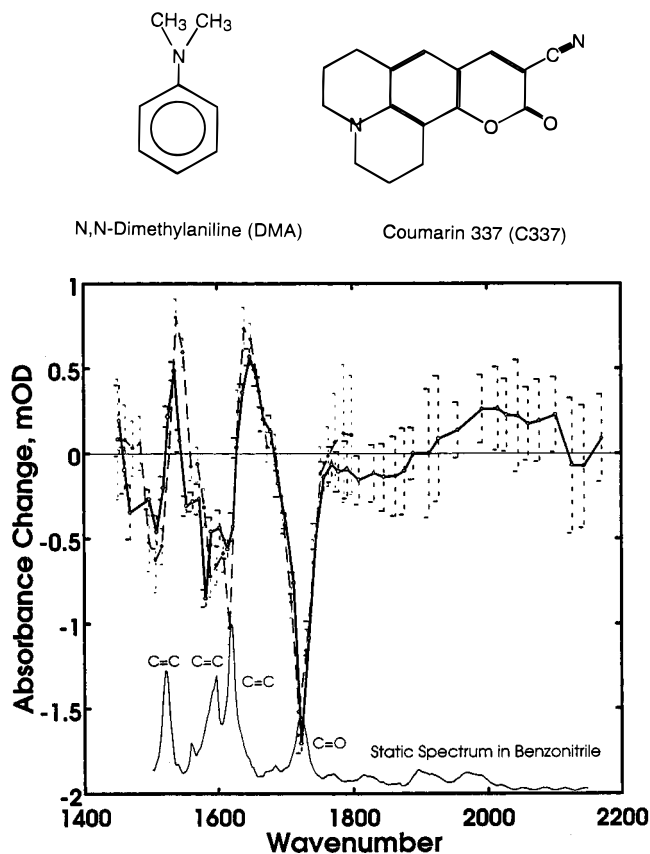


Figure 1. Mid-infrared response to optical excitation of C337 in dichloromethane (dashed line) and benzonitrile (solid line). No electron transfer occurs in these solvents. The solid line with error bars provides a difference spectrum (static absorbance minus absorbance perturbed by the pump pulse, measured at a 5 ps delay between pump and probe pulses.) The rotating sample is 2×10^{-3} M; the pump energy is 0.3 mJ in a 200 μ m diameter spot. Below the difference spectrum is a static absorbance spectrum with characteristic vibrational absorbances as indicated (not to scale).

excited, the quantum yield of fluorescence drops dramatically, e.g., $\Phi_{\text{FL}}(\text{CH}_2\text{I}_2) \sim 250\Phi_{\text{FL}}(\text{DMA})$. We assign the fluorescence-quenching process to electron transfer from DMA to C337. Dimethylaniline is a well-known electron donor. It is energetically favorable to transfer an electron from DMA's HOMO (highest occupied molecular orbital) to the photoexcited C337.

Figure 1 shows an infrared difference spectrum of C337 in benzonitrile at 5 ps delay time after excitation at 400 nm (solid bold line). The absorption maximum for C337 in benzonitrile is found at 449 nm. In benzonitrile electron transfer cannot occur. The lower portion of the figure shows the solvent-subtracted static infrared absorption difference spectrum of C337. Directly above these ground state absorbances may be seen the corresponding bleach signatures ($-\Delta\text{OD}$) that result under electronic excitation. The amplitude of the bleach indicates that about 2% of the ground electronic state population has been excited. Positive values of ΔOD indicate vibrational absorbances of the S_1 coumarin/solvent system. Figure 1 also shows the same difference spectrum collected for C337 in $\text{CH}_2\text{-Cl}_2$ (dashed line). Very similar spectral features are observed, showing that the majority of the response comes from C337 vibrations.

A broad feature is seen at early time from 1700 cm^{-1} to more than 2000 cm^{-1} , see Figure 2. We assign this feature to an $S_N \leftarrow S_1$ transition that disappears rapidly.²⁸

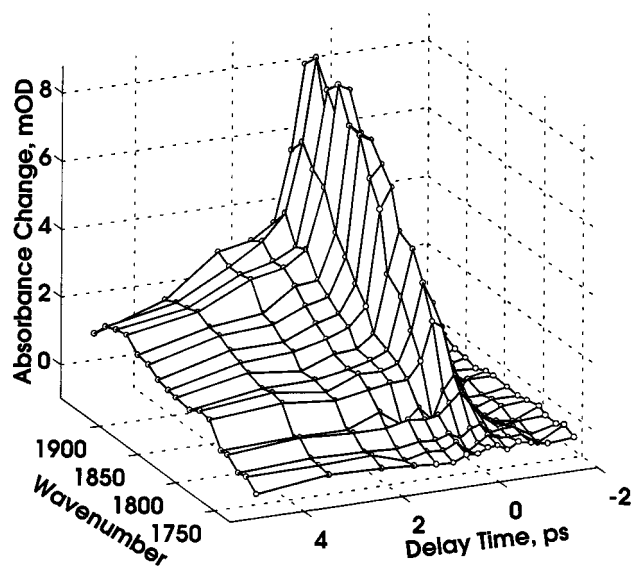


Figure 2. Broad absorbance that rapidly decays is seen above 1750 cm^{-1} . The width of the band is larger than would be expected for a vibrational transition. We assign the absorption to a $S_N \leftarrow S_1$ transition. The disappearance of the absorption is due to vibrational relaxation.

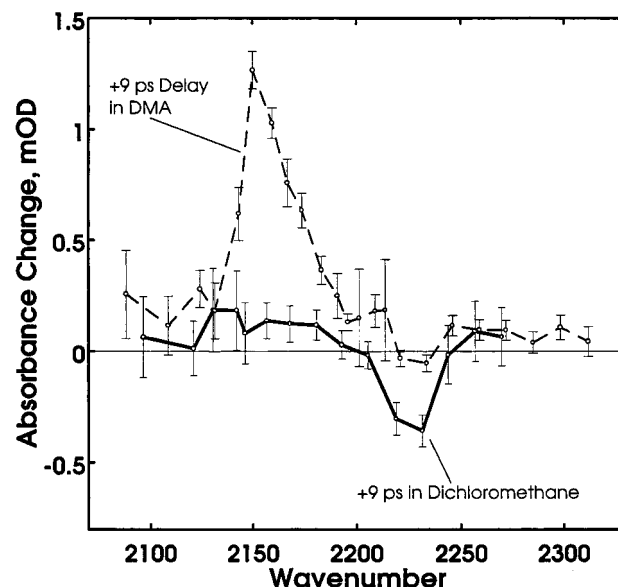


Figure 3. Infrared difference spectra in the region of the nitrile group absorbance of C337 in solution. The solid line is C337 in dichloromethane, in which electron transfer does not occur. The dashed line corresponds to C337 in DMA, in which electron transfer does occur. In both spectra a bleach feature of the ground state C337 is seen at 2230 cm^{-1} . There is an absorption feature visible around 2150 cm^{-1} in DMA at a 9 ps delay that is not visible in dichloromethane. This feature is assigned to the nitrile of the C337 anion.

Figure 3 shows the nitrile absorption region of the difference spectrum in two different solvents. In both cases a bleach of the ground state nitrile absorption is observed near 2230 cm^{-1} . In DMA solution a new, very strong absorbance is seen at 2150 cm^{-1} . This feature is not observed in dichloromethane solution. This region lacks other fundamental or strong overtone absorptions, and we assign the 2150 cm^{-1} band to the nitrile group of the C337 anion. The sharp 2150 cm^{-1} band does not rise instantaneously, but only in several picoseconds, and we associate the appearance of the C337 anion with the band's rise.

Figure 4 shows the 400 nm pump/500 nm probe of the C337 in dichloromethane and dimethylaniline. A clear and persistent gain feature is observed in dichloromethane, whereas the gain rapidly disappears in dimethylaniline. The disappearance of

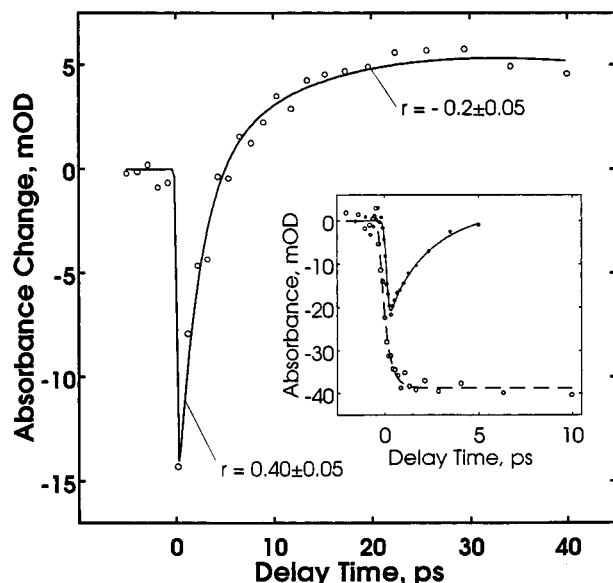


Figure 4. Response of the C337/DMA solution at 500 nm after 400 nm excitation. The data are taken at a frequency where the C337 fluoresces and the DMA radical cation absorbs. In the observed transient absorbance the initial gain (stimulated emission) is replaced by a new absorbance. Also indicated are the anisotropies collected at 0.2 and 30 ps. The early time anisotropy (0.4) corresponds to pumped and probed transition moment vectors, which are approximately parallel. The 30 ps anisotropy (-0.2) corresponds to nearly perpendicular relative orientation of the transition moment vectors. The inset shows 400 nm pump/500 nm probe for C337 in CH_2Cl_2 and DMA, showing the different signals under non-ET and ET, respectively.

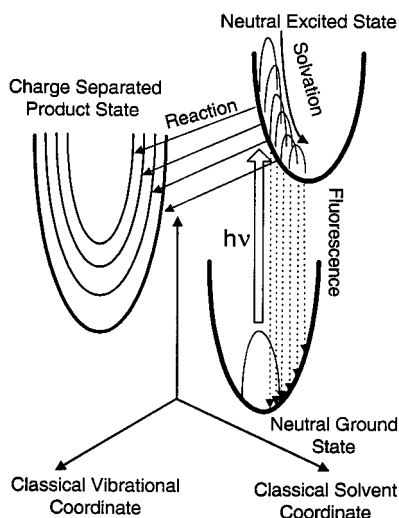


Figure 5. Schematic free energy surfaces. The right-hand side of the figure illustrates the origin of the fluorescence spectrum of C337 in diiodomethane. The initially prepared, neutral excited state experiences complete relaxation of the solvent polarization, and strong fluorescence is observed. When the diiodomethane solvent is replaced by dimethylaniline, a new reaction can occur. This is illustrated by arrows leading to charge separated product state on the left-hand side of the figure. This reaction occurs while solvation is occurring. After ref 14a.

gain is due to loss of S_1 C337 via electron transfer. The ET rate is nonexponential, with an average electron transfer time of 4 ± 0.5 ps. Figure 4 also shows the transient absorption of C337 in DMA at longer times. The gain does not simply disappear but is accompanied by the simultaneous appearance of a new absorbance. The dimethylaniline cation radical shows its absorption maximum at 480 nm, and we assign this transition to that species, consistent with the observed ratio of extinction coefficients.³⁰

The use of parallel and perpendicular relative polarized pump and probe beams permits anisotropy to be measured:

$$r = (I_{\parallel} - I_{\perp}) / (I_{\parallel} + 2I_{\perp})$$

The anisotropy can be related to the ensemble-averaged angle between the pumped and probed transition dipole directions

$$r = (3 \cos^2 \theta - 1) / 5$$

The anisotropies taken at early (0.2 ps) and late (10 and 30 ps) times indicate that the gain spectrum results from the same transition as the optically pumped transition ($r = 0.4 \pm 0.05$), and the new absorption exhibits a transition moment nearly perpendicular to the pumped transition, $r = -0.2 \pm 0.05$. We have also performed visible pump IR probe experiments on the S_0 - S_1 transition moment versus the carbonyl ($r = 0.3$) and nitrile absorbances. These data indicate that the electronic transition moment direction of C337 is long axis polarized, consistent with calculations.²⁹ The transition moment direction of the dimethylaniline radical cation absorption lies parallel to the DMA long axis.³⁰ The anisotropy of $r = -0.2$ indicates that the electron donor and acceptor molecules are aligned with their long axes roughly perpendicular. This measure of the relative orientation of the donor and acceptor in an intermolecular electron transfer complex is novel.

C337 and DMA have 10 and 1.6 D ground state dipole moments, respectively.³¹ Thus, to satisfy the attractive forces, the species could preferentially align. However, the electron transfer rate constant depends on favorable overlap of the HOMO's of C337 and DMA, which is not necessarily optimized by the attractive and repulsive intermolecular interactions. C337 and DMA are of significantly different sizes, and local charge distributions that do not reflect the overall coumarin dipole moment and van der Waals forces may determine solvent packing. Simulations of these orientational preferences and how the donor-acceptor orbital overlap is affected are being pursued. The ground electronic state absorption spectra do not show evidence of preformed ET complexes, for example CT bands.

The thermodynamic parameters for the ET reaction have been estimated as follows. We assume that hexane does not provide any important solvent nuclear orientational polarization contribution to the fluorescence Stokes shift. Since it is not known what the Stokes shift for C337 would be in DMA if no electron transfer occurred, we have estimated its value by a linear regression analysis of the Stokes shift of C337 in 15 solvents of different polarities.³¹ Polarities of the solvents have been determined by the reaction field functionality and by their $E_T(30)$ values.^{13,27,31,32} The use of these two polarity indices and the regression analysis of the fluorescence Stokes shifts predicts the solvent nuclear contribution to the Stokes shift would be 322 cm^{-1} (reaction field index) or 295 cm^{-1} ($E_T(30)$ index). The intramolecular contribution to the Stokes shift is 1541 or 1513 cm^{-1} by these indices. The observed Stokes shift for the real C337/DMA solution is 1675 cm^{-1} , which suggests that ca. 50% of the solvent polarization has developed, if vibrational relaxation has occurred in S_1 . However, this information is inadequate for estimating the Stokes shift because it may be caused by the electron transfer itself, if there are favorable vibronic channels for ET that access particularly nonequilibrium solvation structures of S_1 .^{14,32,34} Irreversible electrochemical measurements show that the reduction potential of C337 in DMA is -2.1 eV versus the SCE electrode.³⁵ The oxidation potential of DMA is ca. 0.7 eV. E_{00} is 2.725 eV, on the basis of the static electronic spectra. From Nagasawa et al.^{14a} we take the value of $E_{ox} - E_{IPS} = -0.2$ eV. Thus the driving force

for the electron transfer, $\Delta G^\circ = -E_{00} + E_{\text{ox}}(\text{solV}^{0/+}) - E_{\text{red}}(\text{dye}^{0/-}) - E_{\text{PS}}$, is ca. -6600 cm^{-1} . It is unlikely that the classical reorganization energy for electron transfer can be comparable, given the weak polarity of DMA and the rigidity of C337. We are pursuing measurements and simulations to examine the role of nonequilibrium vibrations in controlling ET process,³²⁻³⁵ see Figure 5.

References and Notes

- (1) For recent reviews in this area, see: *J. Phys. Chem.* **1996**, *100* (Centennial Issue). (a) Stratt, R. M. *J. Phys. Chem.* **1996**, *100*, 12981. (b) Eisenthal, K. G. *Ibid.* **1996**, *100*, 12997. (c) Voth, G. A.; Hochstrasser, R. M. *Ibid.* **1996**, *100*, 13034. (d) Barbara, P. F.; Meyer, T. J.; Ratner, M. A. *Ibid.* **1996**, *100*, 13148.
- (2) (a) Zusman, L. D. *Z. Phys. Chem.* **1994**, *186*, 1. (b) Zusman, L. D. *J. Chem. Phys.* **1980**, *49*, 295.
- (3) Calef, D. F.; Wolynes, P. G. *J. Phys. Chem.* **1983**, *87*, 3387.
- (4) Sparglione, M.; Mukamel, S. *J. Chem. Phys.* **1988**, *88*, 3265.
- (5) (a) Hynes, J. T. *J. Phys. Chem.* **1986**, *90*, 3701. (b) van der Zwan, G.; Hynes, J. T. *J. Chem. Phys.* **1982**, *76*, 2993.
- (6) (a) Sumi, H.; Marcus, R. A. *J. Chem. Phys.* **1986**, *84*, 4894. (b) Marcus, R. A.; Sutin, N. *Biochim. Biophys. Acta* **1985**, *811*, 265. (c) Marcus, R. A. *J. Chem. Phys.* **1956**, *24*, 966.
- (7) Newton, M. D.; Sutin, N. *Annu. Rev. Phys. Chem.* **1984**, *35*, 437.
- (8) Beratan, D. N. *J. Chem. Phys.* **1988**, *89*, 6195.
- (9) (a) Bixon, M.; Jortner, J. *J. Chem. Phys.* **1993**, *176*, 467. (b) Jortner, J.; Bixon, M. *J. Chem. Phys.* **1988**, *88*, 167. (c) Rips, I.; Klafter, J.; Jortner, J. *J. Chem. Phys.* **1988**, *86*, 4288.
- (10) Bader, J. S.; Kuharski, R. A.; Chandler, D. *J. Chem. Phys.* **1990**, *93*, 230.
- (11) Coalson, R. D.; Evans, D. G.; Nitzan, A. A Nonequilibrium Golden Rule Formula for Electronic State Populations in Nonadiabatically Coupled Systems., preprint.
- (12) Barbara, P. F.; Walker, G. C.; Smith, T. P. *Science* **1992**, *256*, 975.
- (13) Maroncelli, M.; Fleming, G. R. *J. Chem. Phys.* **1987**, *86*, 6221.
- (14) (a) Nagasawa, Y.; Yartsev, A. P.; Tominaga, K.; Bisht, P. B.; Johnson, A. E.; Yoshihara, K. *J. Phys. Chem.* **1995**, *99*, 653. (b) Yoshihara, K.; Tominaga, K.; Nagasawa, Y. *Bull. Chem. Soc. Jpn.* **1995**, *68*, 696.
- (15) Wynne, K.; Galli, C.; Hochstrasser, R. M. *J. Chem. Phys.* **1994**, *100*, 4797.
- (16) Walker, G. C.; Barbara, P. F.; Doorn, S. K.; Dong, Y.; Hupp, J. T. *J. Phys. Chem.* **1991**, *95*, 5712.
- (17) Asahi, T.; Mataga, N. *J. Phys. Chem.* **1992**, *93*, 6575.
- (18) Gould, I. R.; Young, R. H.; Moody, R. E.; Farid, S. *J. Chem. Phys.* **1991**, *95*, 2068.
- (19) Kosower, E. M.; Huppert, D. *Annu. Rev. Phys. Chem.* **1986**, *37*, 127.
- (20) Weaver, M. J.; McManis, G. E., III *Acc. Chem. Res.* **1990**, *23*, 294.
- (21) Simon, J. D.; Doolen, R. *J. Am. Chem. Soc.* **1992**, *114*, 4861.
- (22) Lippert, E.; Rettig, W.; Bonacic-Koutecky, V.; Heisel, F.; Miehle, J. A. *Adv. Chem. Phys.* **1990**, *92*, 7241.
- (23) Nocek, J. M.; Zhou, J. S.; DeForest, S.; Priyadarshy, S.; Beratan, D. N.; Onuchic, J. N.; Hoffman, B. M. Theory and Practice of Electron Transfer Within Protein-Protein Complexes: Application to the Multi-Domain Binding of Cytochrome c by Cytochrome c Peroxidase. Submitted for publication in *Chem. Revs.*
- (24) Jimenez, R.; Fleming, G. R.; Kumar, P. V.; Maroncelli, M. *Nature* **1994**, *369*, 471.
- (25) (a) Mathis, J. R.; Kim, H. J.; Hynes, J. T. *J. Am. Chem. Soc.* **1993**, *115*, 8245. (b) Hynes, J. T. *Nature* **1994**, *369*, 439.
- (26) Akhremichev, B.; Wang, C.; Walker, G. C. *Rev. Sci. Instrum.* **1996**, *67*, 3799.
- (27) Reichardt, C. *Chem. Rev.* **1994**, *94*, 2319.
- (28) McCarthy, P. K.; Blanchard, G. J. *J. Phys. Chem.* **1993**, *97*, 12205.
- (29) Kurnikov, I. Private communication.
- (30) Shida, T.; Nosaka, Y.; Kato, T. *J. Phys. Chem.* **1978**, *82*, 695.
- (31) Abdel-Mottaleb, M. S. A.; Antonious, M. S.; Abo-Aly, M. M.; Ismaiel, L. F. M.; El-Sayed, B. A.; Sherief, A. M. K. *J. Photochem. Photobiol. A* **1989**, *50*, 259.
- (32) Walker, G. C.; Akesson, E.; Johnson, A. E.; Levinger, N. E.; Barbara, P. F. *J. Phys. Chem.* **1992**, *96*, 3728.
- (33) Spears, K. G. *J. Phys. Chem.* **1995**, *99*, 2469.
- (34) Doorn, S. K.; Stoutland, P. O.; Dyer, R. B.; Woodruff, W. H. *J. Am. Chem. Soc.* **1991**, *113*, 1.
- (35) The reduction potential was measured in C337/DMA solutions with added (0.1 M) *t*-butylammonium perchlorate, which resulted in slightly shifted ($<5 \text{ nm}$) absorption and fluorescence spectra compared to C337/DMA solutions without added salt. The absolute magnitude of ΔG° could thus be smaller than we report. H. Shirota, H. Pal, K. Tominaga, K. Yoshihara, work in progress.